AD-A105 902 BRIGHAM YOUNG UNIV PROVO UTAH DEPT OF CHEMICAL ENGI--ETC F/G 9/1
LITHIUM-ALUMINUM ALLOY ELECTRODES IN LITHIUM CHLORATE.(U)
JAN 81 D H SHEN, D N BENNION N00014-80-C-0345
UNCLASSIFIED TR-2 NL

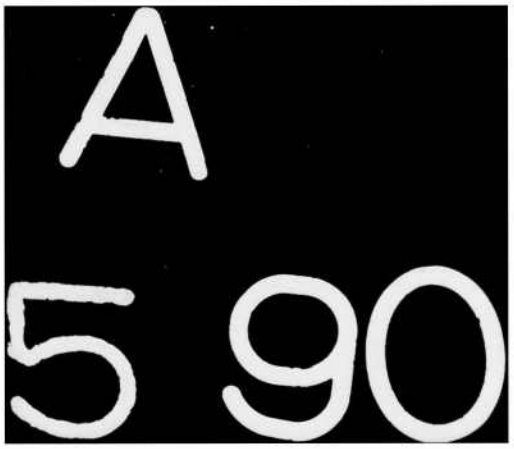
A
5 90

OFFICE OF NAVAL RESEARCH
Contract No. N0014-80-C-0345
Task No. NR 359-551

TECHNICAL REPORT NO. 2

Lithium-Aluminum Alloy Electrodes in Lithium Chlorate

by

David H. Shen and Douglas N. Bennion

Prepared for Publication
in the
Journal of the Electrochemical Society

Brigham Young University

Department of Chemical Engineering

Provo, Utah 84602

January 1981

X

SECURITY CLASSIFICATION OF THIS PAGE (When Data Entered)

REPORT DOCUMENTATION PAGE	READ INSTRUCTIONS BEFORE COMPLETING FORM
1. REPORT NUMBER: Technical Report No. 2	2. GOVT ACCESSION NO. AD-A105 902	3. RECIPIENT'S CATALOG NUMBER
4. TITLE (and Subtitle): Lithium-Aluminum Alloy Electrodes in Lithium Chlorate.	5. TYPE OF REPORT & PERIOD COVERED: Technical Report.
	6. PERFORMING ORG. REPORT NUMBER
7. AUTHOR(s): David H. Shen and Douglas N. Bennion	8. CONTRACT OR GRANT NUMBER(s): N0014-80-C-0345
9. PERFORMING ORGANIZATION NAME AND ADDRESS: Department of Chemical Engr. Brigham Young University Provo, Utah 84602 — work initiated at Univ. of Calif. Los Angeles	10. PROGRAM ELEMENT, PROJECT, TASK AREA & WORK UNIT NUMBERS: NR359-551
11. CONTROLLING OFFICE NAME AND ADDRESS: Office of Naval Research/Chemistry Program Arlington, VA 22217	12. REPORT DATE: January 20, 1981
	13. NUMBER OF PAGES: 20
14. MONITORING AGENCY NAME & ADDRESS (if different from Controlling Office)	15. SECURITY CLASS. (of this report)
	15a. DECLASSIFICATION/DOWNGRADING SCHEDULE

16. DISTRIBUTION STATEMENT (of this Report)

Approved for Public Release. Distribution Unlimited

17. DISTRIBUTION STATEMENT (of the abstract entered in Block 20, if different from Report)

Submitted for publication in Journal of The Electrochemical Society

18. SUPPLEMENTARY NOTES

19. KEY WORDS (Continue on reverse side if necessary and identify by block number)

fused salt
primary battery
reserve battery

20. ABSTRACT (Continue on reverse side if necessary and identify by block number)

To prevent lithium dendrite growth during cycling of Li electrodes in molten $LiClO_3$ at 140°C, a Li-Al electrode in cells of the type $Li/LiClO_3/Li\text{-}Al$ has been investigated. Two discharge plateaus, one about 0.42V and the other about 0.20V versus a lithium wire, were obtained. No lithium dentrites were observed. Continued cycling caused the lithium-aluminum electrode to break down to particles or grains. The corrosion of isolated Al grains during operation of a Li-Al electrode was confirmed using atomic absorption spectrophotometer (AA) analysis on a white precipitate formed where the alloy electrode had been.

DD FORM 1 JAN 73 1473 EDITION OF 1 NOV 65 IS OBSOLETE

403273 LB

SECURITY CLASSIFICATION OF THIS PAGE (When Data Entered)

Lithium-Aluminum Alloy Electrodes in Lithium Chlorate

by

David H. Shen[1] and Douglas N. Bennion[2]

Chemical, Nuclear, and Thermal Engineering Department
University of California, Los Angeles 90024

Abstract

To prevent lithium dendrite growth during cycling of Li electrodes in molten $LiClO_3$ at 140°C, a Li-Al electrode in cells of the type $Li/LiClO_3/LiAl$ has been investigated. Two discharge plateaus, one about 0.42 V and the other about 0.20 V versus lithium wire, were obtained. No lithium dentrites were observed. Continued cycling caused the lithium-aluminum electrode to breakdown to particles or grains. The corrosion of isolated Al grains during operation of a Li-Al electrode was confirmed using atomic absorption spectrophotometer (AA) analysis on a white precipitate formed where the alloy electrode had been.

1) Present address: Jet Propulsion Laboratory, Pasadena, Calif.

2) Present address: Chemical Engineering Dept., Brigham Young Univ.
Provo, Utah 84602

Introduction

A battery system using a lithium negative electrode, an electrolyte of molten lithium chlorate, and an inert nickel positive electrode has been identified (1). In this study, the investigation was focused on using a lithium alloy electrode to stop lithium dendrite formation during lithium deposition. In the operating temperture, 140°C to 150°C, lithium metal is solid. A film exists on the lithium surface which prevents the lithium from contacting the electrolytic solution directly. During charging, lithium ions transfer through the film. The lithium ion transfer rates are different in various places on the film, apparently due to nonuniform thickness of and cracks in the film. The favored lithium deposition sites appear to be the cause of dendrite initiation. An approach to stoping dendrites is to reduce the activity of the deposited lithium by alloying with aluminum and causing the lithium to diffuse into the base material 2, 3, 4.

Experimental

$LiClO_3$ was prepared from $Ba(ClO_3)_2$ and Li_2SO_4 as described by Campbell and Griffiths (5). After dehydration in an argon atmosphere glove box at 50 μm Hg pressure for four weeks at 130°C, the water content in $LiClO_3$ was reduced to less than 0.5%. The final melting point of $LiClO_3$ was between 126°C and 128°C.

Aluminum foil, 99.999% pure, 0.005 inch thick, was purchased from Research Organic/Inorganic Chemical Corporation. It was used for preparing Li-Al working electrodes. Nickel screen, 16 mesh, 0.012 inch wire diameter, was used as the current collector of the working electrode. Litnium ribbon used for both the counter and the reference electrodes was purchased from the Foote Mineral Company. Nickel sheet was used as the backing material for the counter electrodes. Titantium foil was used as lead material for the reference electrode.

A glass pocket cell is shown in Fig. 1. The alloy working electrode and the lithium counter electrode were held in their respective compartments, one inch depth, 3/16 inch and 1/16 inch width respectively. The two compartments contain 1.72 cm^3 and 0.57 cm^3 molten electrolyte respectively. The reference electrode was a lithium wire. A glass rotating disk cell, shown in Fig. 2, was used to conduct the polarization experiments. The Li counter electrode and the Li reference electrode were held in the two glass tube arms of the cell. The aluminum rotating disk was made of a 0.3175 cm (1/8 inch) aluminum rod, with a glass tape sleeve. All experiments were run inside an argon atmosphere glove box. A Perkin Elmer 606 AA spectrophotometer was used to analyze the white precipitate formed on the surface of the alloy electrode. Further details are given elsewhere (6).

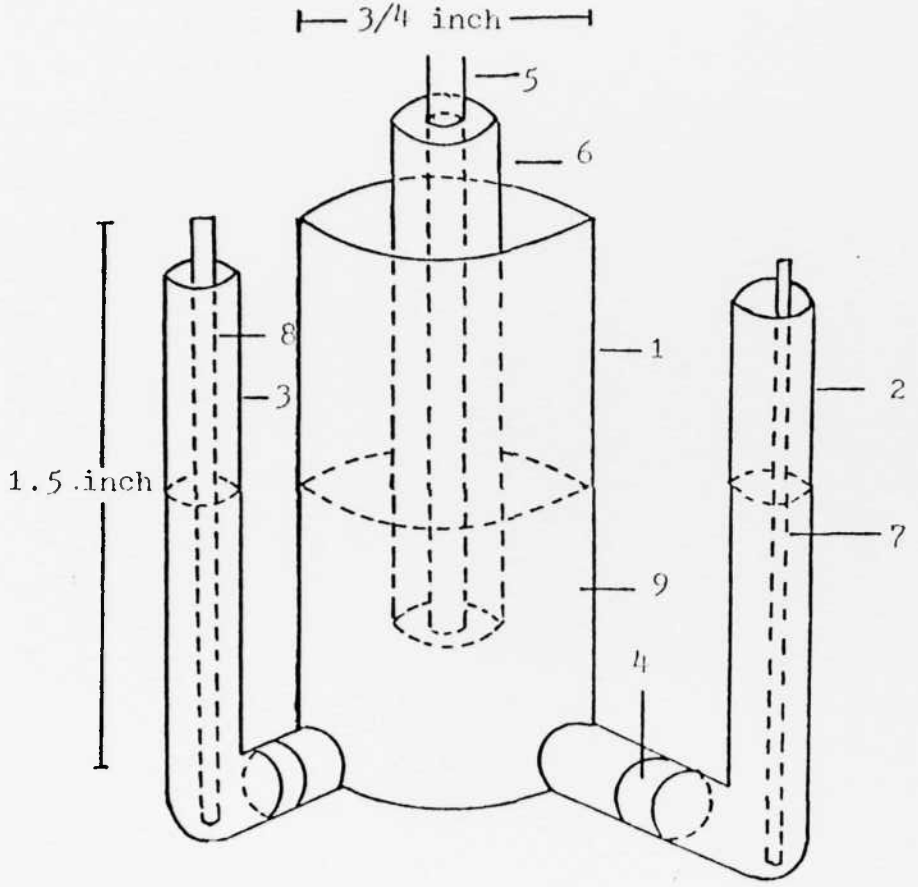

1. glass cylinder
2. glass tube
3. glass tube
4. sintered glass separator
5. Al rod
6. glass tape sleeve
7. Li counter electrode
8. Li reference electrode
9. $LiClO_3$

Figure 2. The cell used in all rotating disk experiments

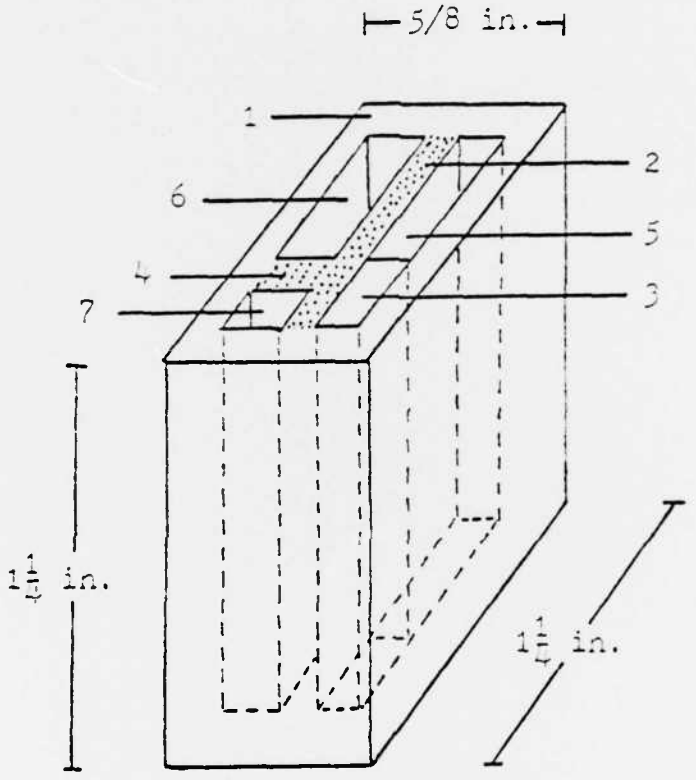

1. glass cell container
2. sintered glass separator
3. pyrex glass block
4. sintered glass block
5. Li counter electrode compartment
6. Li-Al working electrode compartment
7. Li reference electrode compartment

Figure 1. The cell used in all cycling tests.

The alloy electrode used in cycle tests was initially an aluminum foil, 0.05 inch thickness, 1.62 cm x 1.62 cm area, held by two layers of nickel screen, one with a 7 cm long nickel wire as an electrode lead. The pure aluminum electrodes were alloyed electrochemically with lithium. Lithium-aluminum alloy electrodes of four different lithium contents were prepared (A-30%, B-34%, C-51.1%, and D-61.9% lithium on a molar basis) by cathodically charging lithium into the aluminum electrode. The current density for most of the forming was 7.63 mA/cm^2. The potential between the Li-Al working electrode and the lithium reference electrode was measured as a function of time at constant current.

Results and Discussion

The equilibrium emf values of the electrochemically formed lithium-aluminum alloy electrodes (vs. Li^0/Li^+) in molten lithium chlorate electrolyte are given in Fig. 3 as a function of alloy composition (in atom percent lithium).

Electrode C, 51.1% Li, was studied first. During cycling, 600 microequivalents per half cycle, the alloy working electrode was electrically grounded and the current density was 7.63 mA/cm^2. A charge plateau between 0.31 V and 0.33 V was observed. A discharge plateau between 0.37 V and 0.41 V was obtained. After 350 microequivalents charged out of the 8th discharge, the potential rose rapidly to more than 2 V. The electrode had failed. A typical cycle is shown in Fig. 4. Electrode C with 51.1% Li is just into the β phase region; therefore, both the charge and discharge potential are within the $\alpha + \beta$ phase potential. At failure, the discharge potential rose above the potential of the $\alpha + \beta$ phase indicating that the lithium content

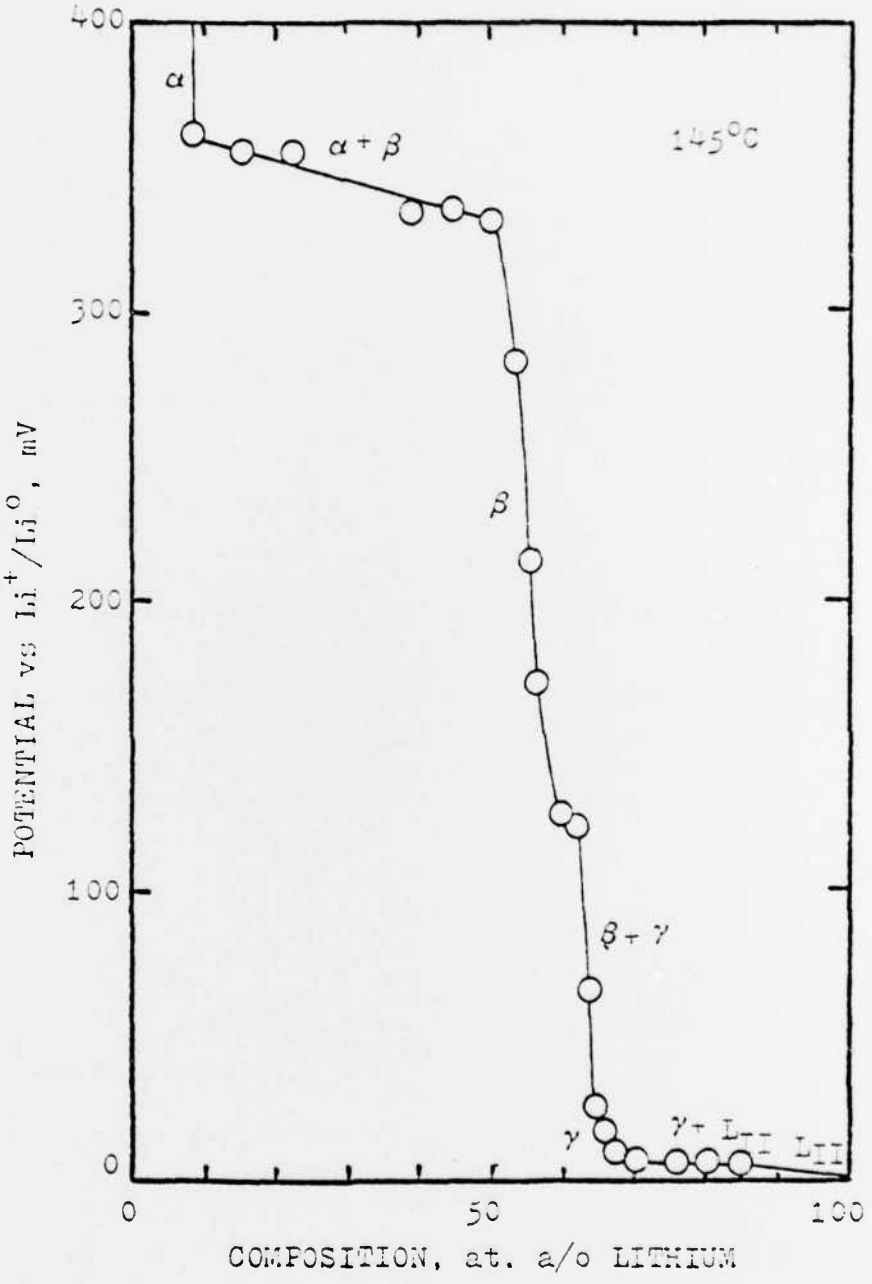

Figure 3. Emf-Composition diagram of lithium-aluminum alloy in molten $LiClO_3$ electrolyte at 418°K

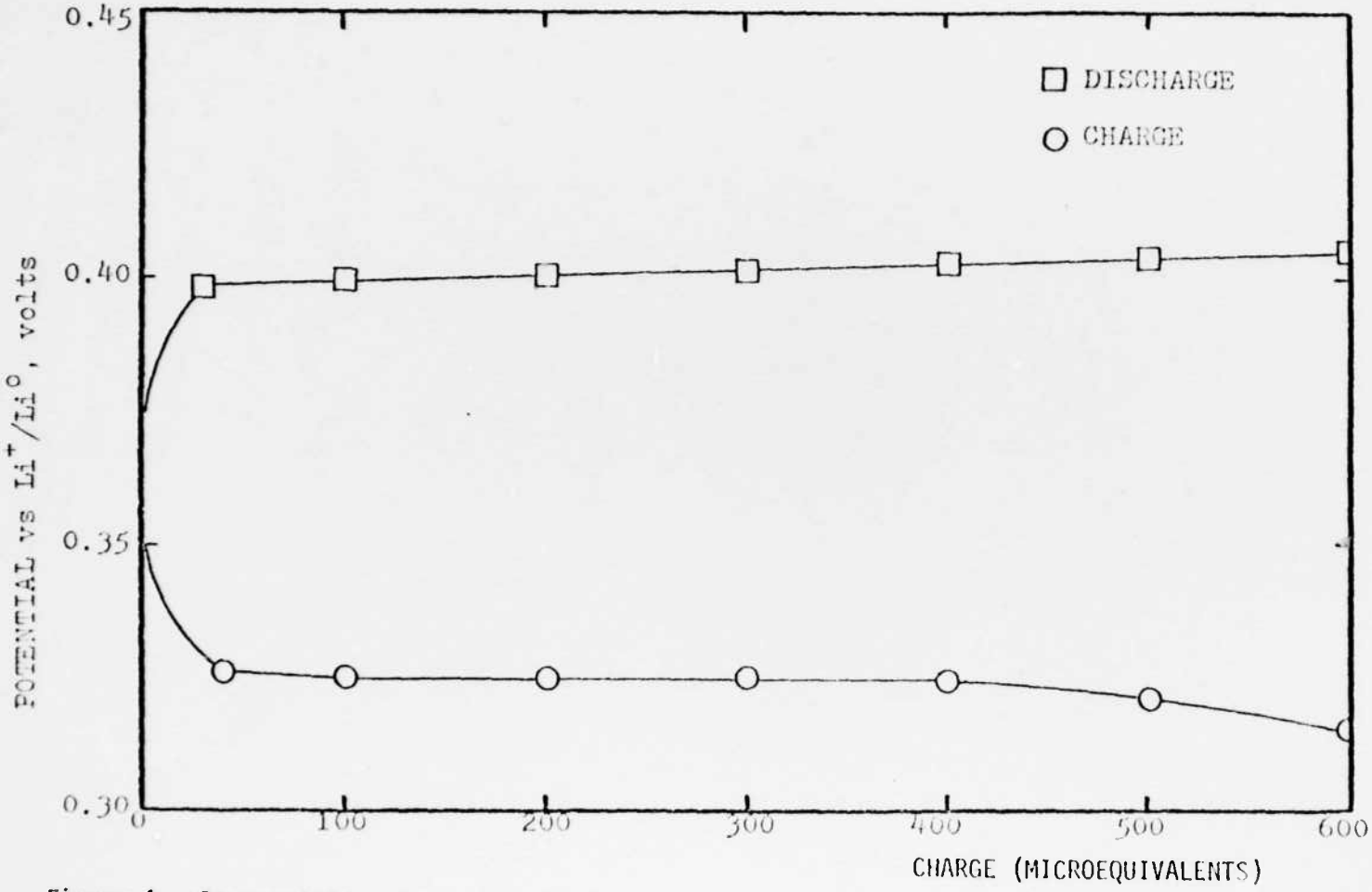

Figure 4. Gavanostatic charge and discharge curves for the cell Li/$LiClO_3$/LiAl (Electrode C, 51.1a/o Li), 600 microequivalents per half cycle, cycle 2, i=7.63 mA/cm^2.

in the Li-Al alloy was below 8.5%

Cycling tests for a type D electrode; 61.9% Li, showed two plateaus during charge and discharge (Figure 5 and 6). The two plateaus imply that the lithium-aluminum alloy is in the $\alpha + \beta$ phase or $\beta + \gamma$ phase. The initial discharge curve at about 0.2 V is characteristic of the $\beta + \gamma$ phase. As cycling progressed, lithium was lost due to corrosion and the composition began switching from $\beta + \gamma$ to $\alpha + \beta$ phase as shown by the 5th discharge cycle in Figure 5. By the 8th discharge, a large part of the cycle was in the $\alpha + \beta$ region characterized by a plateau near 0.4 V. Similar characteristics are demonstrated in Figure 6 for charging, only the curves are shifted a little more negative due to overpotential. The 2nd charging curve is mainly at 0.5 V characteristic of the $\beta + \gamma$ phase between 60 and 63 atom percent lithium. The 6th charging cycle is in between. But by the 9th charge curve much of the charging is at 0.3 V characteristic of the $\alpha + \beta$ phase between 8.5 and 50 mol percent lithium. Only near the end of the charge was the composition approaching the $\beta + \gamma$ composition at the alloy surface. By the 9th cycle, most of the excess lithium initially charged in was corroded away. The length of time required to reach equilibrium was longer after charging than discharging. This result indicates that the surface composition of Li stabalizes faster following discharging compared to charging.

As shown in Tables 1 and 2, the amount of lithium in the forming half cycle and the depth of discharge are the main factors which influence the "life" of a lithium-aluminum electrode. Deep cycles cause more rapid break up of the alloy into small grains and increased corrosion of both the Li and Al by $LiClO_3$.

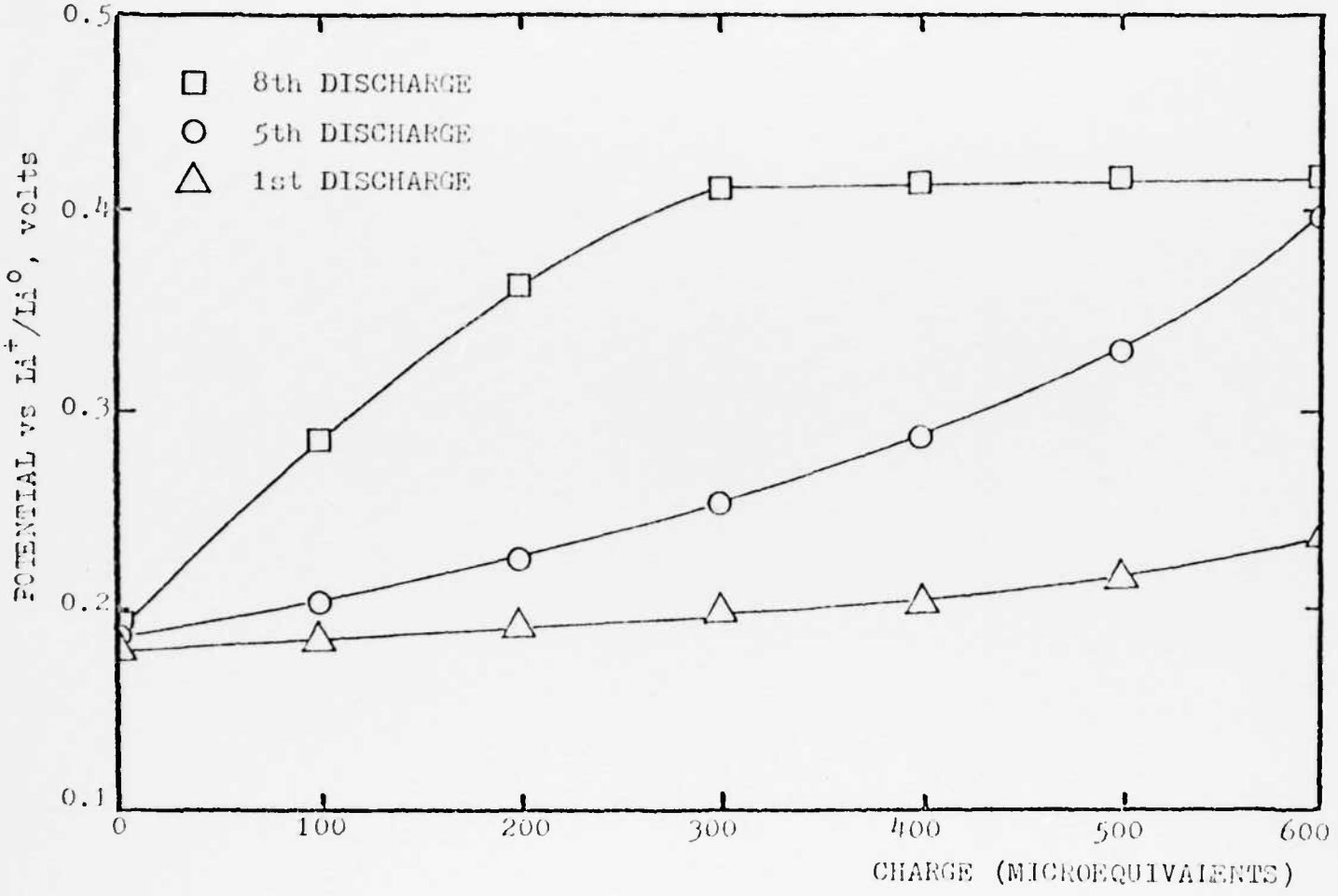

Figure 5. Galvanostatic discharge curves for the cell Li/$LiClO_3$/LiAl (Electrode D, 61.0 a/o Li), 600 microequivalents per half cycle, 1st, 5th, and 8th discharges, i=7.63 mA/cm^2.

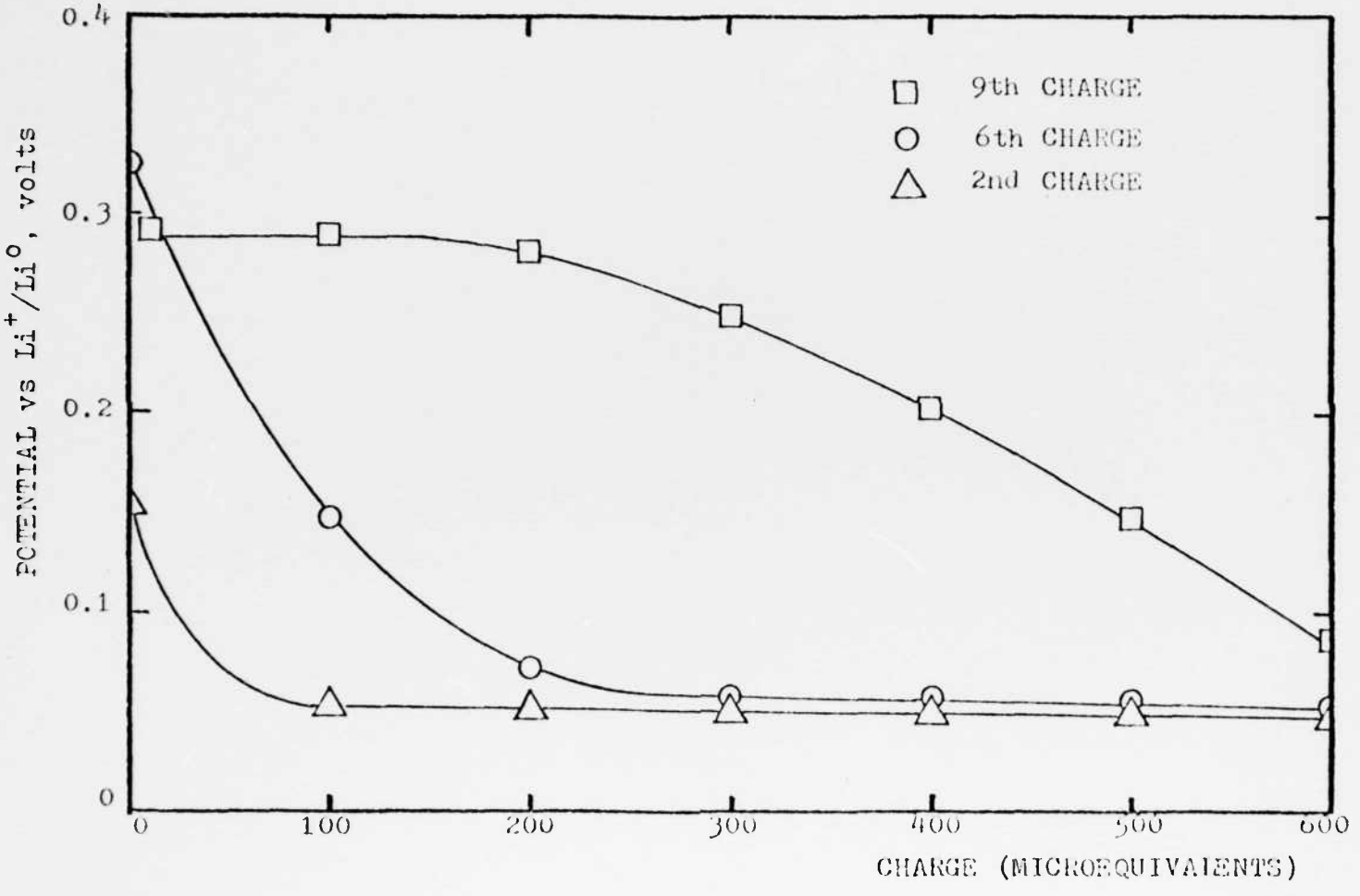

Figure 6. Galvanostatic charge curves for the cell Li/$LiClO_3$/LiAl (Electrode D, 61.9 a/o Li), 600 microequivalents per half cycle, 2nd, 6th, and 9th charges, i=7.63 mA/cm^2.

Table 1. Cycling tests for electrodes B, C, and D with 200 microequivalents per half cycle.

Li atomic content in Li-Al alloys after initial forming half cycle. (a/o Li)	electrode B, 34.0 a/o, $\alpha+\beta$ phase	electrode C, 51.1 β phase	electrode D, 61.9 $\beta+\gamma$ phase
Initial forming charge size (microequivalents)	1667	3280	5413
Capacity used for each charge and discharge half cycle (microequivalents)	200	200	200
% of discharge depth, i.e., 200 microequivalents divided by initial forming charge size	12.0%	6.1%	3.7%
Total amount of charge in (microequivalents)	2675	8406	17813
Total amount of charge out (microequivalents)	1134	5124	12438
Total amount of charge out divided by total amount of charge in times 100%	42.56%	60.96%	69.83%
The number of full cycles	5*	24	59

*: The Li-Al electrode could not charge out 200 microequivalents in the 6th discharge half cycle.

Table 2. Cycling tests for electrode D with various depth per half cycle.

Li atomic content in Li-Al alloys after initial forming half cycle. (a/o Li)	electrode D, 61.9 a/o $\beta+\gamma$ phase	D	D	D
Initial forming charge size (microequivalents)	5413	5491	5413	5688
Capacity used for each charge and discharge half cycle (microequivalents)	200	600	1200	2400
% of discharge depth, i.e., 200 microequivalents divided by initial forming charge size	3.7%	10.9%	22.2%	42.2%
Total amount of charge in (microequivalents)	17813	10945	10213	8088
Total amount of charge out (microequivalents)	12438	5640	5115	4796
Total amount of charge out divided by total amount of charge in times 100%	69.83%	51.53%	50.08%	59.29%
The number of full cycles	59*	9	4	1

*:The Li-Al electrode could not charge out 200 microequivalents in the 60th discharge half cycle.

During cycling, the aluminum structure broke down to grains which lost electrical contact to other grains. A white precipitate was found on the surface where the aluminum foil had been. According to the results of chemical analysis and AA spectropholometer measurements, the white precipitate is aluminum oxide. The reaction is

$$Al + LiClO_3 \rightarrow Al_2O_3 + LiCl$$

An Al_2O_3 film formed on the surface of the aluminum electrode. During charging, the volume of the electrode expanded to expose more fresh aluminum surface, more Al_2O_3 formed and lithium corrosion rates increased and more Li_2O and LiCl formed tending to isolate Al particles. Once the Li corroded out of an isolated particle, the cathodic protection of the lithium was lost and there was nothing to prevent $LiClO_3$ attack on the Al. Apparently Al_2O_3 is very insoluble in $LiClO_3$. Thus, the aluminum can not be replated.

Lithium in a Li-Al electrode could be corroded by molten $LiClO_3$. This was indicated by the open circuit potential rise during hot stand of the Li-Al electrode in molten $LiClO_3$. The corrosion rate decreased with time because a lithium passive film, LiCl and/or Li_2O, was forming on the alloy surface and providing partial protection.

Polarization experiments using a rotating disk were conducted to investigate the electrochemical behavior of a lithium-aluminum electrode. The result, shown in Fig. 7, indicates that the lithium deposition is the reaction on the cathodic polarization curve. The anodic polarization curve is more complicated. The first plateau is associated with the lithium discharge reaction. At the potential of 1.0 V, the lithium passivated and current dropped from 35 mA to 0.2 mA. Aluminum dissolution took place at the potential of 1.4 V,

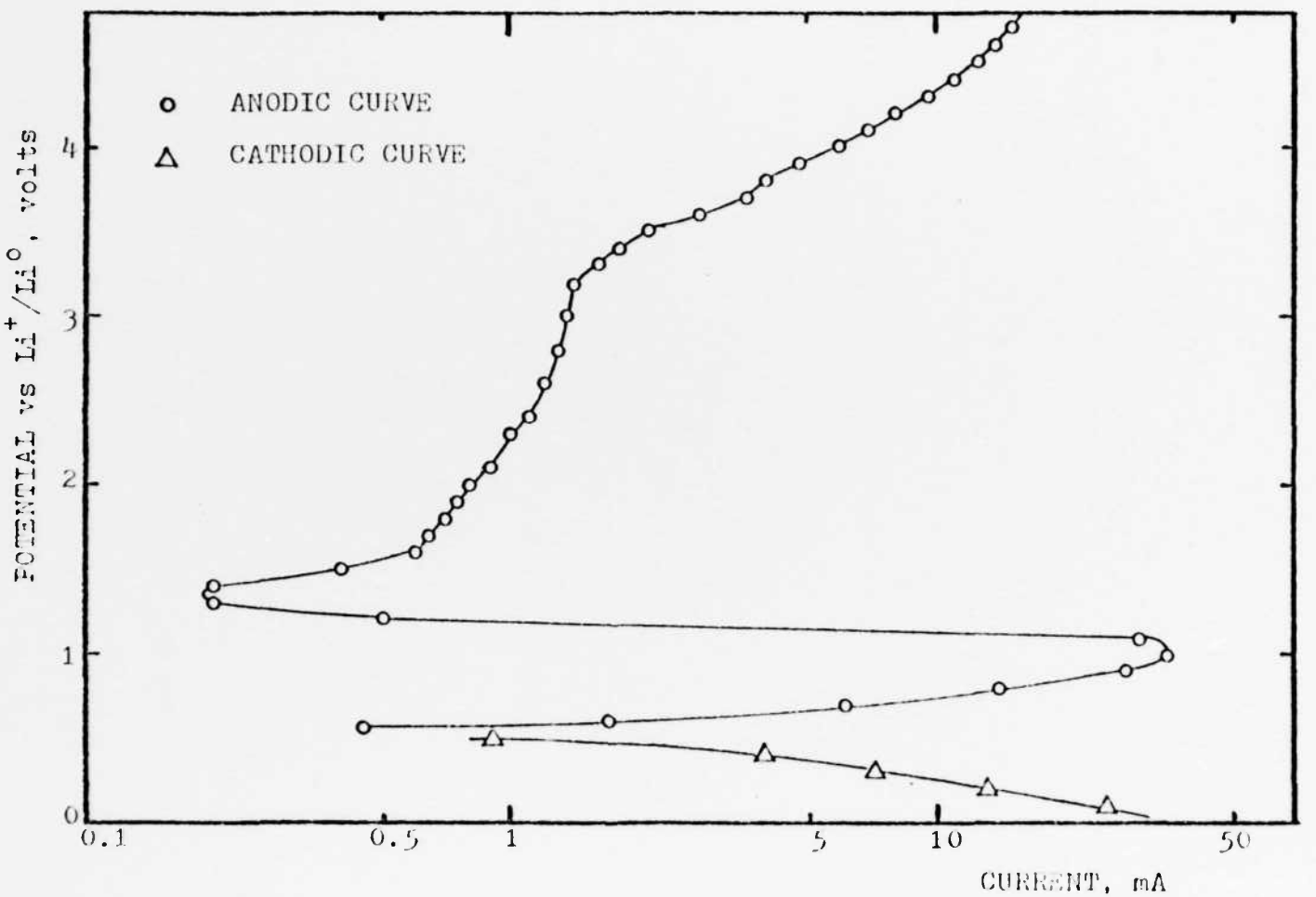

Figure 7. Anodic and cathodic polarization curves of a Li-Al rotating electrode in molten $LiClO_3$ at 145°C.

which is the second discharge plateau. The third plateau, 3.5 V, is oxygen evolution (1).

Figure 8 shows a cyclic voltammogram on a rotating Li-Al electrode in $LiClO_3$ electrolyte. The first oxidation peak, 0.60 V, shows lithium dissolution and corresponds to the reduction peak, 0.20 V, which shows lithium plating. The second oxidation peak, 1.90 V, shows aluminum dissolution, and a smaller cathodic peak, 1.45 V, on the return sweep with the rotating electrode indicates that the oxidation product, assumed to be Al^{+++} (dissolved), is swept away into the solution (7). The small cathodic peak is the only evidence found to show that Al could be deposited on the Li-Al electrodes.

In order to measure the diffusion coefficient of lithium in Li-Al alloy, a potentiostatic pulse method was used. From Fick's 2nd law;

$$\frac{\partial c}{\partial t} = D\frac{\partial^2 c}{\partial x^2}$$

shown below is derived the classic equation

$$I = A\pi F\, C_o\, (\frac{D}{\pi})^{\frac{1}{2}}\, (t)^{-\frac{1}{2}}$$

where C_o is the concentration of lithium in the alloy. The value of C_o was established by charging Li into a pure Al disk. When the potential versus a lithium reference electrode was 360mV, charging was stopped and the Li in Al concentration assumed to be 10 a/o (0.0077 mol/cm^3) based on the potential composition curve shown in Figure 3. Immediately after charging, the potential was potentiostatically set to insure anodic limiting current dissolution of the Li from the alloy but not sufficiently anodic to allow aluminum dissolution. The resulting electrical current was observed as a function of time. A

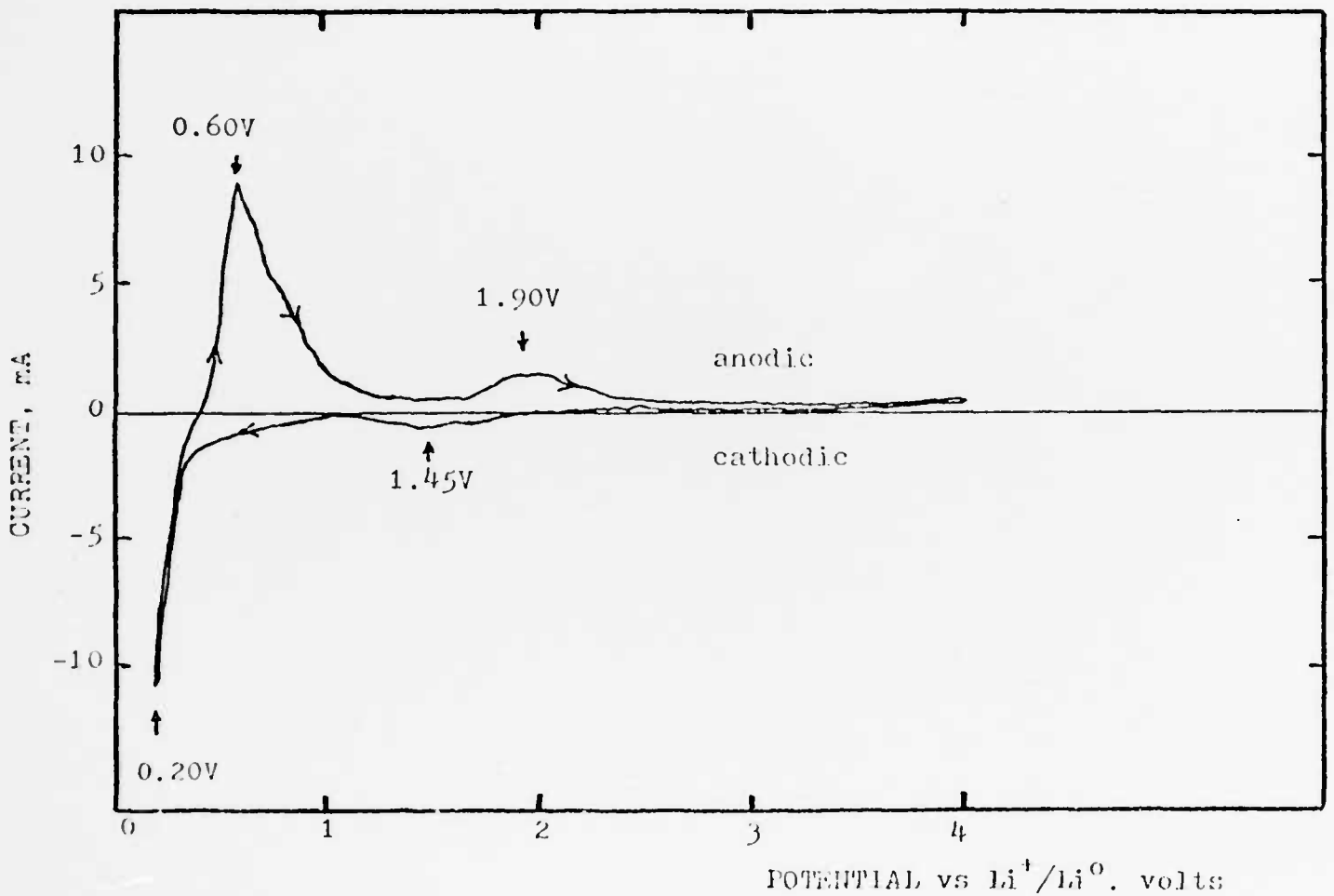

Figure 8. Cyclic voltammogram for a redox reaction on rotating Li-Al electrode in molten $LiClO_3$ at 145°C, sweep rate 12.5mV/sec.

plot of the current versus one over the square root of time yielded a straight line with slope 0.041 $C/s^{0.5}$ (≠). From this slope, the value for the diffusion coefficient of Li in Al at 145°C is 2×10^{-6} cm^2/s, in reasonable agreement with other observations (8,9).

Conclusions

Lithium dendrites occurring during charging on the lithium negative electrode in molten $LiClO_3$ near 140°C can be stopped by using a lithium-aluminum alloy electrode. But the limited "life" of the alloy electrode due to the involvement of the aluminum of the alloy electrode in the cell reaction restrict use of the lithium-aluminum alloy electrode as a stable and reversible negative electrode in lithium chlorate. The corrosion mechanism of Al appears to be isolation of Li-Al alloy grains followed by Li corrosion and then corrosion of the Al grains by $LiClO_3$. A way to control aluminum corrosion is needed.

Acknowledgement

Financial support for this work has been provided by the Office of Naval Research through contract number N0014-80-C-0345.

≠ Fig. 21 of reference 6 shows a slope of 0.00714 $C/s^{0.5}$. An error was found in the data reduction in preparing Fig. 21 of reference 6; 0.041 $C/s^{0.5}$ is the correct value.

References

1. Wang, S.S., "The Electrochemistry of Molten Lithium Chlorate and its Possible Use With Lithium in a Battery," Ph.D. Dissertation, Chemical Engineering Department, University of California, Los Angeles, 1979.

2. Rao, B.M.L., Francis, R.W., and Christopher, H.A., "Lithium-Aluminum Electrode," J. Electrochem. Soc., 124 (10), 1490-1492 (1977).

3. Yao, N.P., Heredy, L.A., and Saunders, R.C., "EMF Measurements of Electrochemical Prepared Lithium-Aluminum Alloy," J. Electrochem. Soc., 118 (7), 1039-1043 (1971).

4. Selman, J.R., DeNuccio, D.K., Sy, C.J., and Steunenberg, R.K., "EMF Studies of Lithium-Rich Lithium-Aluminum Alloys for High-Energy Secondary Batteries," J. Electrochem. Soc., 124 (8), 1160-1164 (1977).

5. Campbell, A.N. and Griffiths, J.E., "The System Lithium Chlorate-Lithium Chlorite-Water at Various Temperatures," Can. J. Chem., 34, 1647 (1956).

6. Shen, D.H., M.S. Thesis, School of Engineering and Applied Science, Chemical Engineering Department, University of California, Los Angeles, 1979.

7. Raleigh, D.O., White, J.T., and Ogden, C.A., "Anodic Corrosion Rate Measurement in LiCl-KCl Eutectic," J. Electrochem. Soc., 126 (7), 1087-1093 (1979).

8. Melendres, C.A., and Sy, C.C., "Structure and Cyclic Discharge Behavior of LiAl Electrodes," J. Electrochem. Soc., 125 (5), 727-731 (1978).

9. James, S.D., "The Lithium Aluminum Electrode," Electrochim Acta, 21, 157-8 (1976).

10. Melendres, C.A., "Kinetics of Electrochemical Incorporation of Lithium into Aluminum," J. Electrochem. Soc., 124, 650-655 (1977).


DATE
ILME